International Journal of Information, Control and Computer Sciences
ISSN: 2517-9942
Vol:3, No:5, 2009

The Study of the Intelligent Fuzzy Weighted Input Estimation Method Combined with the Experiment Verification for the Multilayer Materials

Ming-Hui Lee, Tsung-Chien Chen, Tsu-Ping Yu and Horng-Yuan Jang

***Abstract*—**The innovative intelligent fuzzy weighted input estimation method (FWIEM) can be applied to the inverse heat transfer conduction problem (IHCP) to estimate the unknown time-varying heat flux of the multilayer materials as presented in this paper. The feasibility of this method can be verified by adopting the temperature measurement experiment. The experiment modular may be designed by using the copper sample which is stacked up 4 aluminum samples with different thicknesses. Furthermore, the bottoms of copper samples are heated by applying the standard heat source, and the temperatures on the tops of aluminum are measured by using the thermocouples. The temperature measurements are then regarded as the inputs into the presented method to estimate the heat flux in the bottoms of copper samples. The influence on the estimation caused by the temperature measurement of the sample with different thickness, the processing noise covariance Q, the weighting factor γ, the sampling time interval Δt, and the space discrete interval Δx, will be investigated by utilizing the experiment verification. The results show that this method is efficient and robust to estimate the unknown time-varying heat input of the multilayer materials.

***Keywords*—**Multilayer Materials, Input Estimation Method, IHCP, Heat Flux.

I. Introduction

THE multilayer materials are composed of two or more different kind of materials and have all the characteristic advantages owned by each material. The applications of multilayer materials are widespread as in the electrical, aviation, automobile, ship-building, and physical exercise machine industries. For example, some super conduction materials composed of the multilayer materials have the zero-resistance property at a certain temperature and are widely used. For some electronic chips, such as the central processing units (CPU) or the video cards, often produce heat during the working process. To resolve this situation, the heat-dissipating fins that are made of some kind of multilayer material are then used. However, to prevent the temperature from rising is an important matter to prolong the lifespan and to enhance the stability during the course of development of semiconductor and other electronic devices. In the literature, Yu [1] in 2004 used the fast lagrangian analysis of continua (FLAC) to analyze the heat conduction mechanism under the fixed temperature boundary condition. Hon [2] in 2006 analyzed it by using the fixed flux control instead of the fixed temperature boundary condition, and showed the precision in measuring the physical condition of multilayer materials. The method to deal with the inverse heat conduction problem is called regularization method, which is divided into the universe regularization method (Scott and Beck [3] in 1989) and the conjugate gradient iteration method (Alifanov [4] in 1978 and Mikhailov [5] in 1983). Although the universe regularization method is relatively simpler, it produces higher computational load due to the longer solving time and the increasing number of matrix dimensions. The conjugate gradient iteration method adopts the optimal control concept to solve the inverse heat conduction problem and has the computational structure with higher efficiency. This method was adopted by many researchers such as Huang [6] and Li [7]. Both algorithms are the batch type of off-line processes, which are not very efficient. In the practical use, the parameters should be determined in real time. Therefore, Tuan in 1996 proposed the on-line input estimation algorithm [8] which is compose of the Kalman filter and the recursive least square algorithm. The Kalman filter produces a residual renewal array. The array is then applied to the least square algorithm to estimate the parameters. Since each estimate only requires the output and measurement of the last moment, it will greatly reduce the computational memory load. This method is an on-line recursive input estimation algorithm. It can effectively and precisely estimate the time-varying unknown inputs [9]. Chen in 2008 used an intelligent fuzzy weighting factor to take the place of the weighting function used in the recursive least square algorithm and construct an intelligent fuzzy weighted estimator [10]. This is a inverse

Ming-Hui Lee is with the Department of Civil Engineering, Chinese Military Academy, Fengshan, Kaohsiung, Taiwan, R.O.C. (e-mail: g990406@gmail.com).

Tsung-Chien Chen was with Department of Power Vehicle and Systems Engineering, Chung Cheng Institute of Technology, National Defense University, Ta-His, Tao-Yuan, Taiwan, R.O.C. (e-mail: chojan@ccit.edu.tw).

Tsu-Ping Yu is with the School of Power Vehicle and Systems Engineering Chung Cheng Institute of Technology, National Defense University, Ta-His, Tao-Yuan, Taiwan, R.O.C. (e-mail: johinuee0921@hotmail.com).

Horng-Yuan Jang was with Department of Computer Science and Information Engineering, Nan Kai University of Technology, Taiwan, R.O.C. (e-mail: jghgyn@nkut.edu.tw).

algorithm which has the properties of fast tracking and low affection due to the noise. From the improvements done by Tuan and Chen, such as the on-line input estimation method (IEM), the adaptive input estimation method (AIEM), and the fuzzy weighted input estimation method (FWIEM), to the irregular shaped inverse heat conduction problem [11], the temperature and heat flux estimation of electronic devices [12],the applications of the ballistic estimation, the shooting condition estimation of tank barrels [13], and the load estimation of bridges [14], most of those researches were using numerical simulation with assumed known conditions. This paper will verify the availability of this theorem by using 4 different multilayer material samples, which are compose of one copper sample and one aluminum sample with different thickness. These samples are heated by using the standard heat source from the bottoms. The thermocouples are equipped on the tops of samples to obtain the temperature measurements. The temperature data are then adopted by the intelligent fuzzy weighted input estimation method to estimate the heat flux at the bottoms of the samples. Besides, the influence due to the modeling error variance Q, the weighting factor γ, and the sampling interval Δx is investigated to show the robustness and efficiency of this algorithm.

II. Experiment Equipment

The entire experiment modular includes the signal source, the test samples, the sensors, the data acquisition device, and the computer module. The purpose of experiment is to inversely estimate the temperature and heat flux of the sample by using the temperature measurements of the multilayer material samples surface. Therefore, the multilayer material samples are heated by adopting the standard heat source, and the thermocouples (K type) are equipped on the multilayer material samples surface. Moreover, the data acquisition device is linked with the thermocouples to measure the temperature data. The experiment devices and the samples used are illustrated as follows:

A. The Signal Source

The standard heat source generator with the maximum output power of 200W is compatible with an alternating/direct current power source of 110 volt. The 30VDC power is series connected and can supply stable power to the heater. The standard heat source generator provides heat from its bottom layer. The inner wall and top of this device is insulated. It is a critical technique to perform the experiment in the insulated condition for the direct heat conduction problem. In addition, 5 holes with the diameter of 2mm have been punched on the top of the generator for the thermocouples to measure the surface temperatures of the test samples.

B. The Test Samples

The copper sample is stacked up 4 aluminum samples with different thicknesses. The thickness of copper sample is 5mm. The following thermal properties of the copper are used in the calculation. k =391.1 $W/m\cdot k$, ρ=8940 kg/m^3 , and c_p =386 $J/kg\cdot k$. 4 aluminum samples with different thicknesses of 2mm, 3mm, 4mm, and 5mm are used. The following thermal properties of the aluminum are used in the calculation. k =187 $W/m\cdot k$, ρ =2710 kg/m^3 , c_p =872 $J/kg\cdot k$.

C. Sensors

The thermocouples (K type) are used in this experiment.

D. The Temperature Data Acquisition Device

The device with the type of NI-9211 and the interface of 4 data transmission (NI USB-9162) is manufactured by the National Instruments Company and can be used to implement the signal acquisition, procedure and transformation. It is composed of the high performance measurement and control card, the signal process modular, the filter amplifier, and the electric charge amplifier.

E. The Computer Module (Including the Software Programs)

① Intel *processor* 1.6G computer, the signal express software, and the Matlab programming language can be used to process the signal data.

② The SIGNAL EXPRESS acquisition software: The software in coordination with the data acquisition system developed by the National Instruments Company can collect data from the subject system in real time. The sampling rate, the temperature range, the sampling time, the sensor type, the compensation of the cold junction, the frequency channel, and the record style to record the real-time signal of the system can be configured.

③ The presented method can be programmed by using the Matlab programming language. The temperature measurements are then regarded as the inputs into the method, which is to estimate the heat flux in the bottoms of samples.

III. Mathematical Formulation

Two different kind of multilayer material samples are adopted. The thickness of sample is represented by L . The A_1 (copper) sample has the thickness of L_1, the heat conduction coefficient of k_1, the density of ρ_1, and the specific heat of c_1. The B_2 (aluminum) sample has the thickness of L_2, the heat conduction coefficient of k_2 , the density of ρ_2 , and the specific heat of c_2. The heat conduction interface is assumed to be ideal. This means the heat flux and the temperature at the surface of $x = L_1$ are the same. The standard heat source with flux of $q(t)$ is applied at $x = 0$. The boundary condition of $x = L$ is insulated. By equipping the thermocouple sensor at the position, $x = L$, and measuring the surface temperature of the multilayer materials, the heat-conducting model is formed as shown in Fig. 1.

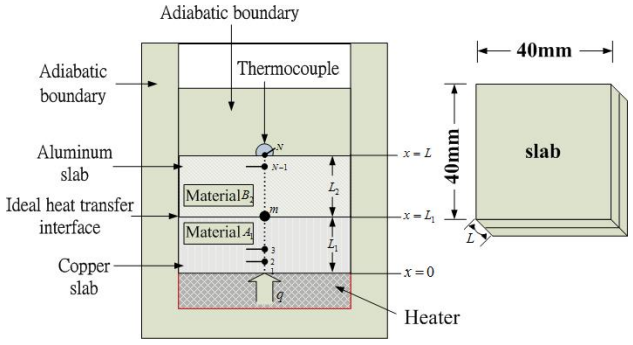

Fig. 1 Heat Transfer Model

The 1-D heat-conducting governing equations are as follows:

$$k_1 \frac{\partial^2 T}{\partial x^2} = \rho_1 c_1 \frac{\partial T}{\partial t} \qquad 0 < x < L_1, 0 < t \le t_f \quad (1)$$

$$-k_1 \frac{\partial T}{\partial x} = q(t) \qquad x = 0, t > 0 \quad (2)$$

$$-k_1 \frac{\partial T}{\partial x} = -k_2 \frac{\partial T}{\partial x}, T|_{A_1} = T|_{B_2} \quad x = L_1 \quad (3)$$

$$k_2 \frac{\partial^2 T}{\partial x^2} = \rho_2 c_2 \frac{\partial T}{\partial t} \qquad L_1 < x < L, 0 < t \le t_f \quad (4)$$

$$-k_2 \frac{\partial T}{\partial x} = 0 \qquad x = L \qquad t > 0 \quad (5)$$

$$T(x,0) = T_0 \qquad 0 \le x \le L \quad (6)$$

$$z(t) = T(x,t) + v(t) \qquad x = L \quad (7)$$

where $T(x,t)$ represents that the temperature is a function of time, t, and the position, x. T_L is the $x = L$ temperature. $z(t)$ is the temperature measurement $v(t)$ is the measurement noise, which is assumed to be the Gaussian white noise with zero mean. T_0 is the initial temperature. The equations (1)~(6) are the heat-conducting governing equations of the multilayer materials. The equation (7) is the measured equation.

The multilayer material sample is separated into N-1 equal portions with the length of Δx. "$i = 1$" is marked at x=0. The temperature is T_1. "$i = m$" is marked at $x = L_1$. The temperature is T_m. "$i = N$" is marked at $x = L$. The temperature is T_N. By using the D`Souza [15] central differential method to substitute Equation (1) in the space derivative and the boundary condition equations (2-5), the heat-conducting governing equations can be transferred as following differential equation. The deduced process can be shown as follows:

$$\frac{\partial T_i}{\partial x} = \frac{T_{i+1} - T_{i-1}}{2\Delta x}, \frac{\partial^2 T}{\partial x^2} = \frac{T_{i+1} - 2T_i + T_{i-1}}{\Delta x^2} \quad (8)$$

when $i = 1$

$$\dot{T}_1(t) = \frac{\partial T_1}{\partial t} = \frac{k_1}{\rho_1 c_1} \frac{\partial^2 T_1}{\partial x^2} = \frac{k_1}{\rho_1 c_1} \frac{T_2 - 2T_1 + T_0}{\Delta x^2} \quad (9)$$

From the boundary condition in equation (2), it is clear that

$$-k_1 \frac{\partial T_1}{\partial x} = -k_1 \frac{T_2 - T_0}{2\Delta x} = q(t)$$

$$T_0 = T_2 + \frac{2\Delta x q(t)}{k_1} \quad (10)$$

By substituting equation (10) to (9) can be rearranged as follows:

$$\dot{T}_1(t) = \frac{2k_1(T_2 - T_1)}{\rho_1 c_1 \Delta x^2} + \frac{2q(t)}{\rho_1 c_1 \Delta x} \quad (11)$$

when $i = 2,3,\ldots,i,\ldots,m-2$ can be obtained as the following equation.

$$\dot{T}_i(t) = \frac{k_1}{\rho_1 c_1} \left(\frac{T_{i+1} - 2T_i + T_{i-1}}{\Delta x^2}\right) \quad (12)$$

The contact point of the two materials, m is the ideal interface of the heat-conduction, then,

$$k_1 \frac{T_{m-1} - T_m}{\Delta x} = k_2 \frac{T_m - T_{m+1}}{\Delta x} \quad (13)$$

$$T_m = \frac{k_1}{k_1 + k_2} T_{m-1} + \frac{k_2}{k_1 + k_2} T_{m+1} \quad (14)$$

when $i = m-1$, the equation (12) can be rearranged as follows:

$$\dot{T}_{m-1}(t) = \frac{k_1}{\rho_1 c_1} \left(\frac{T_m - 2T_{m-1} + T_{m-2}}{\Delta x^2}\right) = \frac{k_1}{\rho_1 c_1 \Delta x^2} \left(T_{m-2} - \frac{k_1 + 2k_2}{k_1 + k_2} T_{m-1} + \frac{k_2}{k_1 + k_2} T_{m+1}\right) \quad (15)$$

when $i = m$, the equation (12) can be rearranged as follows:

$$\dot{T}_m(t) = \frac{k_1}{\rho_1 c_1} \left(\frac{T_{m+1} - 2T_m + T_{m-1}}{\Delta x^2}\right) = \frac{k_1}{\rho_1 c_1 \Delta x^2} \left(\frac{k_1 - k_2}{k_1 + k_2} T_{m+1} + \frac{k_2 - k_1}{k_1 + k_2} T_{m-1}\right) \quad (16)$$

when $i = m+1$, the equation (12) can be rearranged as follows:

$$\dot{T}_{m+1}(t) = \frac{k_2}{\rho_2 c_2} \left(\frac{T_{m+2} - 2T_{m+1} + T_m}{\Delta x^2}\right) = \frac{k_2}{\rho_2 c_2 \Delta x^2} \left(\frac{k_1}{k_1 + k_2} T_{m-1} - \frac{2k_1 + k_2}{k_1 + k_2} T_{m+1} + T_{m+2}\right) \quad (17)$$

when $i = m+2 \cdots N-1$, the equation (12) can be rearranged as follows:

$$\dot{T}_i(t) = \frac{k_2}{\rho_2 c_2 \Delta x^2} (T_{i+1} - 2T_i + T_{i-1}) \quad (18)$$

when $i = N$, the equation (12) can be rearranged as follows:

$$\dot{T}_N(t) = \frac{k_2}{\rho_2 c_2 \Delta x^2} (T_{N+1} - 2T_N + T_{N-1}) \quad (19)$$

From the boundary condition in equation (5), it is clear that

$$-k_2 \frac{\partial T_N}{\partial x} = -k_2 \frac{T_{N+1} - T_{N-1}}{2\Delta x} = 0 \quad (20)$$

$$T_{N+1} = T_{N-1} \quad (21)$$

By substituting equation (21) to (19) can be rearranged as follows:

$$\dot{T}_N(t) = \frac{2k_2}{\Delta x^2 \rho_2 c_2} T_{N-1} - \frac{2k_2}{\Delta x^2 \rho_2 c_2} T_N \quad (22)$$

From the equations (11, 12, 15-18, 22) and the fictitious process noise input, the one-dimensional continuous-time state equation can be obtained as the following:

$$\dot{T}(t) = AT(t) + Bq(t) + G(t)w(t) \quad (23)$$

$$T(t) = \{T_1(t), T_2(t), \ldots, T_m(t), \ldots, T_N(t)\}^T \quad (24)$$

$$B = \begin{bmatrix} \frac{2}{\Delta x \rho_1 c_1} \\ 0 \\ 0 \\ \vdots \\ \vdots \\ 0 \end{bmatrix} \quad (25)$$

Let $\alpha_1 = \frac{k_1}{\rho_1 c_1 \Delta x^2}$, $\alpha_2 = \frac{k_2}{\rho_2 c_2 \Delta x^2}$, then, the state matrix, A is shown as follows:

$$A = \begin{bmatrix} -2\alpha_1 & 2\alpha_1 & 0 & \cdots & & & 0 & \cdots & & \cdots 0 \\ \alpha_1 & -2\alpha_1 & \alpha_1 & 0 & \cdots & & \cdots & & & \cdots 0 \\ 0 & \alpha_1 & -2\alpha_1 & \alpha_1 & 0 & \cdots & 0 & \ldots & & \cdots 0 \\ \vdots & & \ddots & \ddots & & & & & & \\ 0 & \cdots & & \alpha_1 & A_{m-1,m-1} & 0 & A_{m-1,m+1} & 0 & \cdots & \cdots 0 \\ \vdots & & \cdots & 0 & A_{m,m-1} & 0 & A_{m,m+1} & 0 & \cdots & \cdots 0 \\ & & \cdots & 0 & A_{m+1,m-1} & 0 & A_{m+1,m+1} & \alpha_2 & \cdots & \cdots 0 \\ \vdots & 0 & \cdots & & & 0 & \alpha_2 & -2\alpha_2 & \alpha_2 & \cdots 0 \\ 0 & & 0 & \cdots & & \ddots & \ddots & \ddots & \ddots & \cdots 0 \\ 0 & 0 & \cdots & & & 0 & \cdots & 0 & A_{N,N-1} & A_{N,N} \end{bmatrix} \quad (26)$$

$$A_{m-1,m-1} = -\alpha_1 \frac{k_1 + 2k_2}{k_1 + k_2}, \quad A_{m-1,m+1} = \alpha_1 \frac{k_1}{k_1 + k_2},$$

$$A_{m,m-1} = -\alpha_1 \frac{k_2 - k_1}{k_1 + k_2}$$

$$A_{m,m+1} = \alpha_1 \frac{k_1 - k_2}{k_1 + k_2}, \quad A_{m+1,m-1} = \alpha_2 \frac{k_1}{k_1 + k_2},$$

$$A_{m+1,m+1} = -\alpha_2 \frac{2k_1 + k_2}{k_1 + k_2}$$

$$A_{N,N-1} = 2\alpha_2, \quad A_{N,N} = -2\alpha_2$$

where A is the state matrix, B and C are the input matrices. $w(t)$ is assumed to be the Gaussian white noise with zero mean, and it represents the modeling error. The continuous-time state equation (23), can be discretized with the sampling time, Δt. The discrete-time state equation and its relative equations are shown as follows.

$$T(k+1) = \Phi[(k+1)\Delta t, k\Delta t]T(k) + \Gamma(k+1)q(k) + w(k+1) \quad (27)$$

where

$$\Phi[(k+1)\Delta t, k\Delta t] = e^{A\Delta t}$$

$$\Gamma(k+1) = \int_{k\Delta t}^{(k+1)\Delta t} \Phi[(k+1)\Delta t, \tau] B(\tau) d\tau$$

$$w(k+1) = \int_{k\Delta t}^{(k+1)\Delta t} \Phi[(k+1)\Delta t, \tau] G(\tau) w(\tau) d\tau$$

In the equations above, $w(k)$ is the processing error input vector, which is assumed to be the Gaussian white noise with zero mean and with the variance, $E\{w(k)w^T(j)\} = \mathrm{Q}\delta_{kj}$. δ_{kj} is the Dirac delta function. The discrete-time measurement equation is shown below.

$$z(k) = HT(k) + v(k) \quad (28)$$

where Z(k) is the observation vector at the kth sampling time. The measurement matrix, $H = [0\ 0 \ldots\ldots 1]$. $v(k)$ is the measurement error vector, which is assumed to be the Gaussian white noise with zero mean and with the variance, $E\{v(k)v^T(j)\} = R\delta_{kj}$.

IV. The Intelligent Fuzzy Weighted RLSE Input Estimation Approach

The conventional input estimation approach has two parts: one is the Kalman filter without the input term, and the other is the fuzzy weighted recursive least square estimator. The system input is the unknown time-varying heat flux. The Kalman filter is operating under the setting of the processing error variance, Q, and the measurement error variance, R. It is to use the difference between the measurements and the estimated values of the system temperature as the functional index. Furthermore, by using the fuzzy weighted recursive least square algorithm, the heat flux can be precisely estimated. The detailed formulation of this technique can be found in Ref [16].

A. The equations of the Kalman filter are shown as follows:

$$\bar{X}(k/k-1) = \Phi \bar{X}(k-1/k-1) \quad (29)$$

$$P(k/k-1) = \Phi P(k-1/k-1)\Phi^T + Q \quad (30)$$

$$s(k) = HP(k/k-1)H^T + R \quad (31)$$

$$K(k) = P(k/k-1)H^T s^{-1}(k) \quad (32)$$

$$P(k/k) = [I - K(k)H]P(k/k-1) \quad (33)$$

$$\bar{Z}(k) = Z(k) - H\bar{X}(k/k-1) \quad (34)$$

$$\bar{X}(k/k) = \bar{X}(k/k-1) + K(k)\bar{Z}(k) \quad (35)$$

B. The recursive least square algorithm:

$$B(k) = H[\Phi M(k-1) + I]\Gamma \quad (36)$$

$$M(k) = [I - K(k)H][\Phi M(k-1) + I] \quad (37)$$

$$K_b(k) = \gamma^{-1} P_b(k-1)B^T(k)\left[B(k)\gamma^{-1}P_b(k-1)B^T(k) + s(k)\right]^{-1} \quad (38)$$

$$P_b(k) = \left[I - K_b(k)B(k)\right]\gamma^{-1}P_b(k-1) \quad (39)$$

$$\hat{q}(k) = \hat{q}(k-1) + K_b(k)\left[\bar{Z}(k) - B(k)\hat{q}(k-1)\right] \quad (40)$$

$$\hat{X}(k/k-1) = \Phi\hat{X}(k-1/k-1) + \Gamma\hat{q}(k) \quad (41)$$

$$\hat{X}(k/k) = \hat{X}(k/k-1) + K(k)\left[Z(k) - H\hat{X}(k/k-1)\right] \quad (42)$$

$\hat{q}(k)$ is the estimated input vector. $P_b(k)$ is the error covariance of the estimated input vector. γ is the weighting constant or weighting factor. *B(k)* and *M(k)* are the sensitivity matrices. $K_b(k)$ is the correction gain. $\bar{Z}(k)$ is the bias innovation produced by the measurement noise and the input disturbance. $s(k)$ is the covariance of the residual. P is the filter's error covariance matrix.

C. The construction of the intelligent fuzzy weighting factor:

The fuzzy weighting factor is proposed based on the fuzzy logic inference system. It can be operated at each step based on the innovation from the Kalman filter. It performs as a tunable parameter which not only controls the bandwidth and magnitude of the RLSE gain, but also influences the lag in the time domain. To directly synthesize the Kalman filter with the estimator, this work presents an efficient robust forgetting zone, which is capable of providing a reasonable compromise between the tacking capability and the flexibility against noises. In the recursive least square algorithm, $\gamma(k)$ is the weighting factor in the range between 0 and 1. The weighting factor $\gamma(k)$ is employed to compromise between the upgrade of tracking capability and the loss of estimation precision. The relation has already been derived as follows ([17]):

$$\gamma(k) = \begin{cases} 1 & \left|\bar{Z}(k)\right| \le \sigma \\ \dfrac{\sigma}{\left|\bar{Z}(k)\right|} & \left|\bar{Z}(k)\right| > \sigma \end{cases} \quad (43)$$

The weighting factor, $\gamma(k)$, as shown in Equation (43) is adjusted according to the measurement noise and input bias. In the industrial applications, the standard deviation σ is set as a constant value. The magnitude of weighting factor is determined according to the modulus of bias innovation, $\left|\bar{Z}(k)\right|$. The unknown input prompt variation will cause the large modulus of bias innovation. In the meantime, the smaller weighting factor is obtained when the modulus of bias innovation is larger. Therefore, the estimator accelerates the tracking speed and produces larger vibration in the estimation process. On the contrary, the smaller variation of unknown input causes the smaller modulus of bias innovation. In the meantime, the larger weighting factor is obtained according to the small modulus of bias innovation. The estimator is unable to estimate the unknown input effectively. For this reason, the intelligent fuzzy weighting factor for the inverse estimation method which efficiently and robustly estimates the time-varying unknown input will be constructed in this research.

The intelligent fuzzy weighted input estimation method is derived following as:

The range of fuzzy logic system input, $\theta(k)$, may be chosen in the interval, $[0,1]$. The input variable is defined as:

$$\theta(k) = \frac{\left|\dfrac{\Delta\bar{Z}(k)}{\bar{Z}(k)}\right|}{\sqrt{\left(\dfrac{\Delta\bar{Z}(k)}{\bar{Z}(k)}\right)^2 + \left(\dfrac{\Delta t}{t_f}\right)^2}} \quad (44)$$

where $\Delta\bar{Z}(k) = \bar{Z}(k) - \bar{Z}(k-1)$. Δt is the sampling interval. t_f is the measure total time. The proposed intelligent fuzzy weighting factor uses the input variable $\theta(k)$ to self-adjust the factor $\gamma(k)$ of the recursive least squares estimator. Therefore, the fuzzy logic system consists of one input and one output variables. The range of input, $\theta(k)$, may be chosen in the interval, $[0,1]$, and the range of output, $\gamma(k)$, may also be in the interval, $[0,1]$. The fuzzy sets for $\theta(k)$ and $\gamma(k)$ are labeled in the linguistic terms of EP (extremely large positive), VP (very large positive), LP (large positive), MP (medium positive), SP (small positive), VS (very small positive), and ZE (zero). The specific membership is defined by using the Gaussian functions.

A fuzzy rule base is a collection of fuzzy IF-THEN rules:

IF $\theta(k)$ is zero (ZE), THEN $\gamma(k)$ is an extremely large positive (EP);

IF $\theta(k)$ is a very small positive (VS), THEN $\gamma(k)$ is a very large positive (VP);

IF $\theta(k)$ is a small positive (SP), THEN $\gamma(k)$ is a large positive (LP);

IF $\theta(k)$ is a medium positive (MP), THEN $\gamma(k)$ is a medium positive (MP);

IF $\theta(k)$ is a large positive (LP), THEN $\gamma(k)$ is a small positive (SP);

IF $\theta(k)$ is a very large positive (VP) THEN $\gamma(k)$ is a very small positive (VS);

IF $\theta(k)$ is an extremely large positive (EP) THEN $\gamma(k)$ is zero (ZE),

where $\theta(k) \in U$ and $\gamma(k) \in V \subset R$ are the input and output of the fuzzy logic system, respectively. Therefore, the nonsingleton fuzzier can be expressed as the following equation:

$$\mu_A(\theta(k)) = \exp\left(-\frac{\left(\theta(k) - \bar{x}_i^l\right)^2}{2\left(\sigma_i^l\right)^2}\right) \quad (45)$$

$\mu_A(\theta(k))$ decreases from 1 as $\theta(k)$ moves away from $\bar{x}_i^l$. $\left(\sigma_i^l\right)^2$ is a parameter characterizing the shape of $\mu_A(\theta(k))$.

The Mamdani maximum-minimum inference engine was used in this paper. The max-min-operation rule of fuzzy implication is shown below:

$$\mu_B(\gamma(k)) = \max_{j=1}^{c}\left\{\min_{i=1}^{d}\left[\mu_{A_i^j}(\theta(k)), \mu_{A_i^j \to B^j}(\theta(k), \gamma(k))\right]\right\} \quad (46)$$

where c is the fuzzy rule, and d is the dimension of input variables.

The defuzzier maps a fuzzy set B in V to a crisp point $\gamma \in V$. The fuzzy logic system with the center of gravity is defined below:

$$\gamma^*(k) = \frac{\sum_{l=1}^{n} \bar{y}^l \mu_B(\gamma^l(k))}{\sum_{l=1}^{n} \mu_B(\gamma^l(k))} \quad (47)$$

n is the number of outputs. $\bar{y}^l$ is the value of the lth output. $\mu_B(\gamma^l(k))$ represents the membership of $\gamma^l(k)$ in the fuzzy set B. Substituting $\gamma^*(k)$ of Equation (47) in Equations (38) and (39) allows us to configure an adaptive fuzzy weighting function of the recursive least square estimator (RLSE). A flow chart of the computation for the application of the intelligent fuzzy weighted input estimation method is shown in Fig. 2.

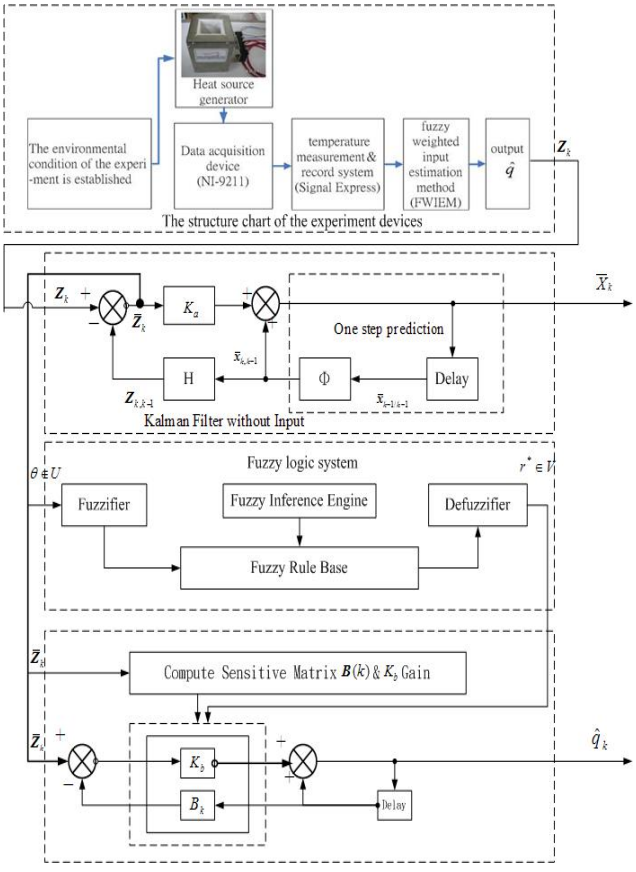

Fig. 2 A flow chart of the computation for the application of the intelligent fuzzy weighted input estimation method

V. Discussion of the Experimental Measurement and Estimation Results

To verify the estimated performance of the proposed method, an inverse heat conduction problem of the multilayer materials is considered. The heat flux in the bottom and temperature are estimated inversely by measuring the temperature on the top. The test sample is heated by the standard heat source with the fixed power. The copper test sample is heated in the bottom; moreover, an aluminum test sample is put on the top of the copper test sample. Two materials are combined with each other tightly. Therefore, the contact point of the two materials is the ideal interface of the heat-conduction. The inner wall and the top of the environment are insulated. The temperature of different thickness (copper fixed $L_1 = 5mm$ and aluminum is $L_2 = 2,3,4,5mm$) test samples are measured by the thermocouples. The total time period, $t_f = 250$ sec. The sampling interval, $\Delta t = 0.5$ sec. The measurement temperature curves of different test samples are shown in Fig. 3.

The temperature measurement from the Fig. 3, it shows that the measurement error of the thermocouple is approximately ±0.01% (with the measurement noise covariance, $R = 10^{-4}$). The space interval, $\Delta x = x_s / N$ (N =30). The process noise covariance matrix, $Q = 10^3$. The temperatures are measured on the tops of different samples with different thicknesses (L=7, 8, 9 and 10mm). Fig. 4 shows that the heat flux, $\hat{q}$ in the bottom is estimated inversely by substituting the temperature data into the presented method. The estimation results demonstrate that the penetration delay of temperature may exist in the estimation process. Since the standard heat source is not in an absolutely insulated condition in the measurement process, in order to reduce the influence of the penetration delay of temperature, 100 data are averaged to ensure the accuracy of the heat flux estimation. The data are selected from the smoothest curve (50sec) of Figs. 4a~4d. The average value of the estimated heat flux, $\hat{q}_{ave} = (\sum_{i=1}^{100} \hat{q}_i)/100$, where the average value of the measured data (150~200sec) from the 7mm test sample, $(\hat{q}_{ave})_1$ =4139.307 W/m^2, the average value of the measured data (190~240sec) from the 8mm test sample, $(\hat{q}_{ave})_2$ =4008.050 W/m^2, the average value of the measured data (195~245sec) from the 9mm test sample, $(\hat{q}_{ave})_3$ =4044.381 W/m^2 , and the average value of the measured data (200~250sec) from the 10mm test sample, $(\hat{q}_{ave})_4$ =4153.028 W/m^2 . The total average value was estimated by the average value of all test samples:

$$\hat{q}_{t\_ave} = \frac{\sum_{i=1}^{4} (\hat{q}_{ave})_i}{4} = 4086.192 \ W/m^2 \quad (48)$$

The total average value of the heat flux is regarded as the heat source in the bottoms of the test samples. In this paper, the

percentage error (PE) is used to verify the precision of the estimation model. The definition of the PE is described in Equation (49).

$$PE(\%) = \left| \frac{\left[\hat{q}_{t\_ave} - (\hat{q}_{ave})_i \right]}{\hat{q}_{t\_ave}} \right| \times 100\% \quad (49)$$

where $\hat{q}_{t\_ave}$ is the total average value of the heat flux. $(\hat{q}_{ave})_i$ is the average value of the ith test sample's heat flux. $i = S_1, S_2, S_3, S_4$, which represent 4 test samples with different thicknesses ($L = 7,8,9,10mm$). The verified comparisons of estimated results are shown as the Table I.

Table I shows that the errors are all small. This means the estimation method can precisely estimate the heat flux for different samples. Besides, the data of the $L = 9mm$ sample are regarded as a reference for adjusting the values of parameters in the estimation method.

TABLE I
THE VERIFIED COMPARISONS OF ESTIMATED HEAT FLUXES

	$L = 7mm$	$L = 8mm$	$L = 9mm$	$L = 10mm$
The average value of the estimated heat flux	4139.307 W/m^2	4008.050 W/m^2	4044.381 W/m^2	4153.028 W/m^2
The percentage error	$PE = 1.29\%$	$PE = 1.91\%$	$PE = 1.02\%$	$PE = 1.63\%$

The Kalman filter is operating under the setting of the processing error variance, Q, and the measurement error variance, R. It regards the renewal values produced by using the difference between the temperature estimates and the temperature measurements as the functional index, and utilizes the real-time least square algorithm to precisely estimate the heat flux. The measurement error variance of the thermocouple is assumed as a given value, $R = 10^{-4}$. The processing error variance, Q is adjusted between 10^{-1} to 10^{9}. The temperature measurements are then regarded as the inputs into the presented method, which estimates the heat flux (195~245sec) in the bottom of multilayer materials sample, $L = 9mm$ (copper sample is 5mm and aluminum sample is 4mm). The relative root mean square error (RRMSE) of the estimated result can be calculated and chosen as the optimal estimation parameters. The definition of the RRMSE is described in Equation (50).

$$RRMSE = \sqrt{\frac{\sum_{s=1}^{n} [(\hat{q}_{t\_ave} - \hat{q}_s)/\hat{q}_{t\_ave}]^2}{n}} \quad (50)$$

where n is the total number of time steps. $\hat{q}_{t\_ave}$ is the actual heat flux. $\hat{q}_s$ is the estimated heat flux. The RRMSE values of the estimation results can be plotted as shown in Fig. 5. It indicates that when the process noise variance, Q increases, it will accelerate the estimation speed and produce the better estimation result. On the other hand, when the process noise variance, Q decreases, the error covariance matrix will decrease, and the Kalman gain $K(k)$. will therefore decrease. The main reason is that the correction need is decreasing, and only the smaller Kalman gain $K(k)$ is needed to offer that correction. On the other hand, as the process noise variance Q increases, the error covariance matrix will increase, which causes the Kalman gain $K(k)$ to increase. The main reason is that the correction need is increasing, and therefore the larger Kalman gain $K(k)$ is needed to offer that correction. As a result, the Kalman filter will have faster correction performance but have larger oscillation in the estimation process.

Fig. 5 shows the increasing modeling error when $Q = 10^{-1} \sim 10^{3}$. This makes the new measurements significant for the correction of estimation. The RRMSE is then reduced. However, if the modeling error is too large ($Q = 10^{4} \sim 10^{9}$), the Kalman filter will produce larger oscillations, which cause the increase of the RRMSE value. As a result, the relatively smaller value of RRMSE is making the parameter $Q = 10^{3}$ the best choice. $Q = 10^{-1}$, 10^{3}, and 10^{6} in Fig. 6a are used to show that when the error is larger, the result with the larger oscillation and faster response will be produced. $Q = 10^{-1}$ in Fig. 6b shows that the temperature curve cannot be estimated precisely.

The estimation results of the heat flux using the constant weighting factors ($\gamma = 0.125, 0.525, 0.925$) and the intelligent fuzzy weighting function are plotted in Fig. 7. The intelligent fuzzy weighting factor $\gamma(k)$ plays the role of the controller, which is employed to compromise between the tracking capability and the loss of estimation precision. When the constant weighting factor ($\gamma = 0.125$) is adopted, the estimation convergence is fairly rapid. The only issue is that the oscillations are also produced. When the constant weighting factor ($\gamma = 0.925$) is adopted, the estimation convergence is fairly slow. However, the oscillation issue in this case is relatively small. As a result, the value of constant weighting factor should be appropriately chosen to obtain better estimation performance, and it will not be easy. The simulation results demonstrate that the fuzzy weighted input estimation inverse methodology can resolve this issue and produce better results in tracking the heat flux.

Considering the influence caused by the sampling interval, N is set to be 18, 30, 45, 90, and 270 to investigate the estimation results. When set $R = 10^{-4}$ and $Q = 10^{3}$, the result is shown in Fig. 8. When Δx is smaller, the computational load is higher, but the result is more precise. On the other hand, when Δx is larger, the result is less precise.

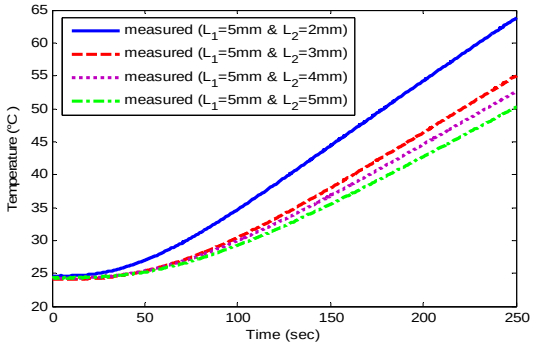

Fig. 3 The curves of temperature measurements. ($L = 7mm$, $8mm$, $9mm$ and $10mm$)

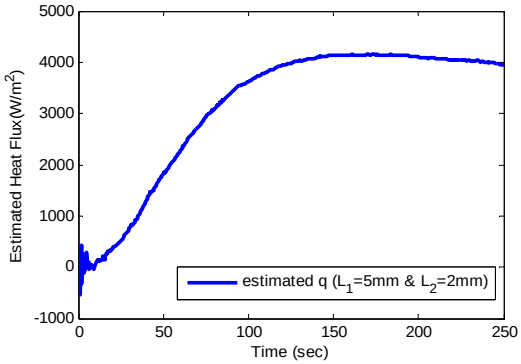

Fig. 4a The estimated heat flux ($L = 7mm$)

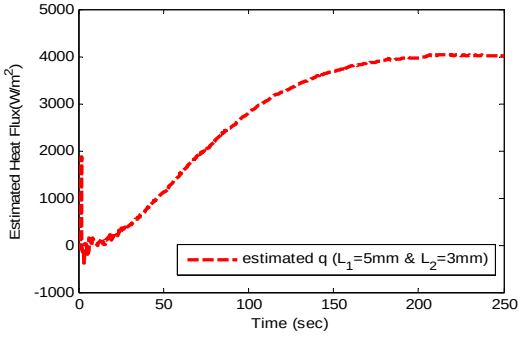

Fig. 4b The estimated heat flux ($L = 8mm$)

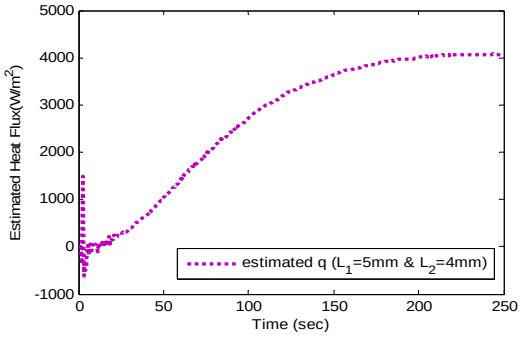

Fig. 4c The estimated heat flux ($L = 10mm$)

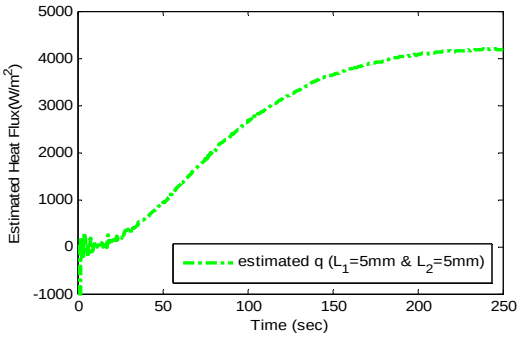

Fig. 4d The estimated heat flux ($L = 9mm$)

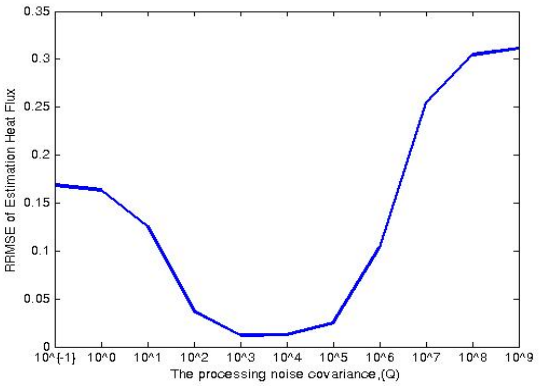

Fig. 5 The RRMSE vs. The different values of Q, ($R = 10^{-4}$)

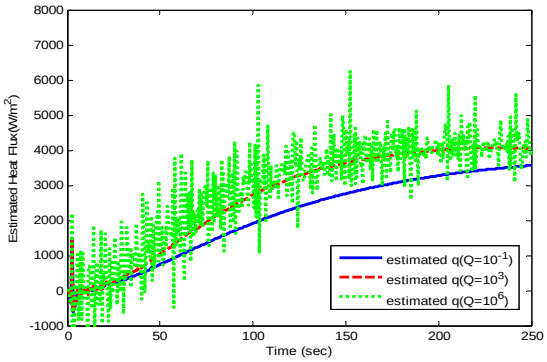

Fig. 6a The estimation results of the heat flux. ($Q = 10^{-1}$, 10^{3} , and 10^{6})

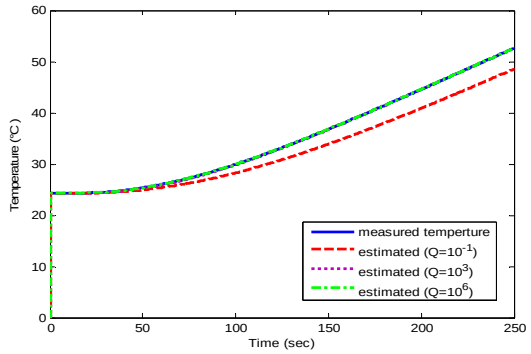

Fig. 6b Comparison of temperature estimates when the values of error variance are different

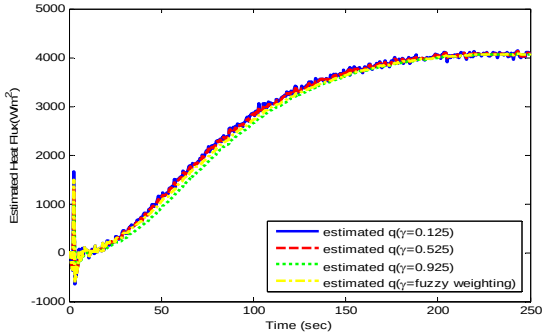

Fig. 7 The estimation results of the heat flux (γ =0.125, 0.525, 0.925 and the fuzzy weighting function)

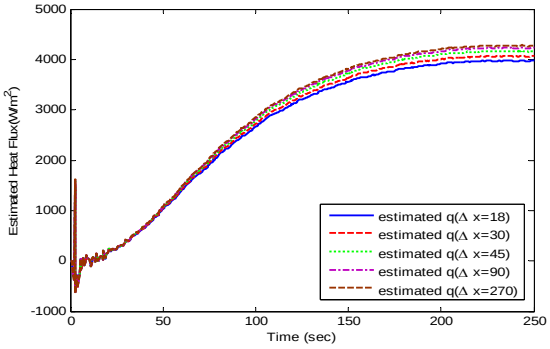

Fig. 8 The estimation results of the heat flux (Δx =18, 30, 45, 90 and 270)

VI. Conclusion

In this paper, the bottoms of the multilayer material test samples with different thicknesses are heated by applying the standard heat source, and the temperatures on the top are measured by using the thermocouples. The FWIEM is utilizing the measured temperature data to estimate the heat flux in the bottoms of samples. The influence on the estimation caused by the processing noise covariance Q, the weighting factor γ, the space interval Δx, will be investigated by utilizing the experiment verification. The results reveal that if the process noise variance Q increases and the smaller weighting factor is adopted, the faster estimation convergence and larger oscillations will be produced. The adoption of fuzzy weighting factor can enhance the speed of tracking and reduce the influence due to the noise. With smaller sampling interval Δx, the computational load will be higher, but the result will be more precise. The experiment verification shows that the FWIEM has the properties of better targat tracking capability and more effective noise reduction, and that it is an efficient, adaptive, and robust inverse estimation method for the estimation of the unknown heat flux of the multilayer material.

Acknowledgment

This work was supported by the National Science Council of the Republic of China under Grant NSC97-2221-E-606-029.

References

[1] Yu, G. H. "A Study of the Thermal Conductive Behaviors of Composite Materials with Double Layers," Department of Construction Engineering, National Kaohsiung First University of Science and Technology, Master Paper, 2004.
[2] Hon, R. L. "A Study of the Thermal Conductive Behaviors of Double Composite Layers with Constant Heat," Department of Construction Engineering, National Kaohsiung First University of Science and Technology, Master Paper, 2006.
[3] Scott, E. P. and Beck, J. V., "Analysis of Order of The Sequential Regularization Solutions of Inverse Heat Conduction Problem," Trans. ASME, Vol. 111, pp.218-224 (1989).
[4] Alifanov, O. M., and Millhailov, V. V., "Solution of the Nonlinear Inverse Thermal Conduction Problem," Journal of Engineering Physics, Vol. 35, No. 6, pp.1501-1506 (1978).
[5] Millhailov, V. V., "Questions of The Convergence of Iteration Methods of Solving The Inverse Heat Conduction Problem," Journal of Engineering Physics, Vol. 45, No. 5, pp.1263-1266 (1983).
[6] Huang, C. H. and Ozisik, M. N., "Inverse Problem of Determining Unknown Wall Heat Flux in Laminar Flow Through a Parallel Plat Duct, "Numerical Heat Transfer, Part A, Vol. 21, pp.55-70 (1992).
[7] Li, H. Y. and Yan, W. M., "Inverse Convection Problem for Determining Wall Heat Flux in Annular Duct Flow," Journal of Heat Transfer Transactions of the ASME, Vol. 122, pp.460-464 (2000).
[8] Tuan, P. C., Fong, L. W., and Huang, W. T., "Analysis of On-Line Inverse Heat Conduction Problems," Journal of Chung Cheng Institute of Technology, Vol. 25(1), pp. 59-73 (1996).
[9] Tuan, P. C., Fong, L. W., and Huang, W. T., "Application of Kalman Filtering with Input Estimation Technique to ON-Line Cylindrical Inverse Heat Conduction Problems," JSME International Journal, Series B, Vol. 40(1), pp. 126-133 (1997).
[10] Chen, T. C. and Lee, M. H., "Intelligent fuzzy weighted input estimation method applied to inverse heat conduction problems," International Journal of Heat and Mass Transfer, Vol.51, pp.4168–4183, 2008.
[11] Chen, T. C. and Hsu S. J.,"A Study of the Gun Barrel Temperature Measurement and Heat Flux Estimation Using Non-destruction Ballistic Experimental Method," Journal of explosives and propellants, R.O.C., Vol.22, No.2, pp. 19-35, 2006.9.
[12] Chen, T. C., and Hsu, S. J., "Input Estimation Method in the Use of Electronic Device Temperature Prediction and Heat Flux Inverse Estimation," Numerical Heat Transfer, Part A, Vol. 52, No. 9, pp. 1-21, 2007.
[13] Chen, T. C., and Hsu, S. J., "Research on the Heat Flux Estimation and Active Heat-dissipation Control of the Barrel Structure," Journal of explosives and propellants, R.O.C., Vol.23, No.2, pp. 13-32, 2007.
[14] Chen, T. C., and Lee, M. H., "Research on Moving Force Estimation of the Bridge Structure using the Adaptive Input Estimation Method," Electronic Journal of Structural Engineering (EI), Vol.8, pp. 20-28, 2008
[15] D'Souza, N. "Numerical Solution of One-dimensional Inverse Transient Heat Conduction by Finite Difference Method, " ASME Paper 75-WA/HT-81, 1975.

[16] Tuan, P. C., Ji, C. C., Fong, L. W., Huang, W. T., "An input estimation approach to on-line two dimensional inverse heat conduction problems, Numerical Heat Transfer B29 (1996) 345-363.
[17] Tuan, P. C. and Hou, W. T., "The Adaptive Robust Weighting Input Estimation for 1-D Inverse Heat Conduction Problem," Numerical Heat Transfer, Part B, Vol.34, pp. 439-456, 1998.

Ming-Hui Lee received his Master's degree in civil Engineering, Ping-Dong Institute of Technology, R.O.C. in 2003, and received Ph.D. degree at Chung-Cheng Institute of Technology, R.O.C. in 2009. Presently, he is an Assistant Professor in the Department of Civil Engineering, Chinese Military Academy, Taiwan, R.O.C. He has worked on inverse problems, estimation theory, structure dynamics, etc.

Tsung-Chien Chen received his MS and Ph. D., both from the Chung Cheng Institute of Technology, Taiwan, in 1994 and 2005. He had served in Department of Systems Engineering at the Chung Cheng Institute of Technology, Taiwan, from 1991 to 2006. Presently, he is Professor in Department of Power Vehicle and Systems Engineering of Chung Cheng Institute of Technology. His research areas include: Estimation theory, inverse problems, control theory, tracking system, optimal control of heat-dissipating, etc.

Tsu-Ping Yu (Graduate student) holds relevant work of maintenance of radar in the missile troop from 1998 to 2007; study the master's degree in motive force of Institute of Technology of National Defense University and System Engineering Research Institute from 2008 to the present. His study directions include estimation theory and heat-conduction problem, etc.

Horng-Yuan Jang was born in Kinmen, Taiwan, 1958. He received the M.Sc. degree in 1984 and the Ph. D. degree in 1998, both in system engineering from Chung Cheng Institute of Technology, Taiwan. He had served in Department of Computer Science and Information Engineering at the Nan Kai University of Technology, Taiwan, since 2000. His current research interests include controller design, estimation technique, and optimal on-line heat-dissipation control methodology.